Lasers in Manufacturing Conference 2015

Influences of Process Parameters on Deposition Width in Laser Engineered Net Shaping

NIU Fangyong[a], MA Guangyi[a], CHAI Dongsheng[a], ZHOU Siyu[a], WU Dongjiang[a,*]

[a]*Key Laboratory for Precision and Non-traditional Machining Technology of Ministry of Education, Dalian University of Technology, Dalian 116024, China*

Abstract

Process parameters have great influence on deposition width in laser engineered net shaping. However, due to the complexity in fabrication process, the relationships of process parameters and deposition width are difficult to figure out quantitatively. Based on energy and mass balance of deposition layers, this study proposed a process model about layer deposition width, which involves the main process parameters of laser engineered net shaping. This model clearly reveals the relationships between deposition width and laser power, scanning speed and powder flow rate. The model shows that the layer deposition width is proportional to $P^{1/2}$ and inversely proportional to $v^{1/2}$, but has almost no relationship with the powder flow rate. The conclusions from the proposed model were verified by the deposition of several 316L stainless steel single-bead wall structures.

Keywords: additive manufacturing, laser engineered net shaping, process parameter, deposition width;

1. Introduction

Laser engineered net shaping (LENS) is a promising additive manufacturing technology that can be used for building three-dimensional components directly from CAD models by layer-wise deposition (Atwood et al.,1998; Keicher et al., 1997). Compared with traditional subtractive machining, many process steps, such as casting, forging and rough machining, are needless for LENS. Therefore, LENS is generally considered as a rapid manufacture technology and has been widely utilized in military and civil fields, such as aerospace

* Corresponding author. Tel.: +86-411-84707625; fax: +86-411-84707625.
E-mail address: djwudut@dlut.edu.cn.

industry (Arcella and Froes, 2000), biomedical research (Bandyopadhyay et al., 2009) and mould manufacturing (Mazumder et al., 2000).

As a rapid manufacture technology, dimensional accuracy of fabricated component is one of the most concerned quality in LENS and extensive studies have proved that the process parameters influences it greatly. Srivastava et al. (2000) investigated the influence of laser power, scan-rate and powder flow rate on the build width of TiAl alloy single-bead wall structures. Their results showed that the build width decreased continuously with increase in the scanning speed and powder flow rate, while increased with increasing in the laser power. Zhang et al. (2007) and Li et al. (2003) found the same laws by fabrication of nickel-based super alloy and 316L stainless steel respectively. De Oliveira et al. (2005) discussed the correlations between the main process parameters and geometrical characteristics of an individual laser track and found that the laser track width W statistically correlates with $P/v^{1/2}$. Generally, rough empirical results could be gotten by experimental analysis in the aforementioned researches. In addition, the process parameters scope discussed by experimental method is usually limited, which can't reflect the real complete relationship between the deposition dimensions. As a result, the numerical relationship revealed by experimental analysis is not accurate enough for quantitative control in LENS process.

This paper deals with the typical shaping procedures of LENS and the cross-sectional profiles of single-bead wall structures. Process model of deposition width is deduced based on mass and energy balance. We then discuss the relationship between main process parameters and deposition width quantitatively. The proposed theory is verified by deposition of 316L stainless steel single-bead wall structures.

2. Deduction of the deposition width model

2.1. Depostion process of LENS

Fig.1(a) shows the cross-section of a 316L stainless steel single-bead wall structure which fabricated by reciprocating deposition (laser power 1000 W, scanning speed 6 mm/s, powder flow rate 0.266 g/s). From Fig. 1(a), it can be found that cross-section morphology of the top layer is a semi-circle which may be resulted from the material's viscosity and surface tension. Accordingly, the deposition width can be considered as two times of radius of the top layer (as shown in Fig. 1(a)). Approximately parallel stripes formed by layer-wise deposition also could be observed. Space between two adjacent stripes agrees well with the set Z-increment which is much smaller than the height of the top layer. This means volume of the top layer is larger than that of a previous layer.

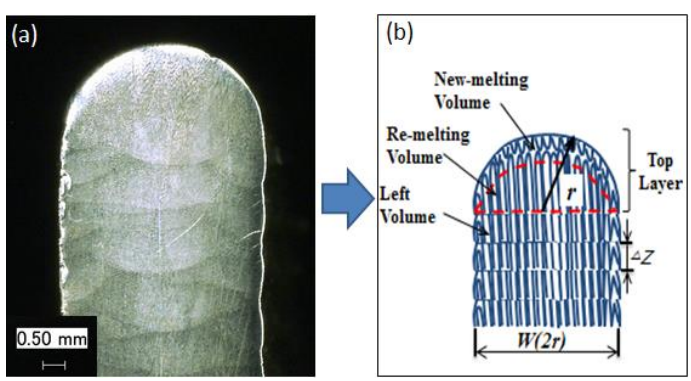

Fig. 1 (a) Cross-section of a 316L stainless steel single-bead wall structure; (b) Schematic of the deposition process of LENS

With some simplification, the schematic of the deposition process of LENS and the geometric characteristic of the cross-section could be obtained as shown in Fig. 1(b). When depositing a new layer, initial molten pool should be formed by re-melting of the previous layer so as to catch sending powders. Then the caught powders are melted to increase the volume of the molten pool as well as the fabricating single-bead wall structure. As a result, the top layer can be considered consisting of a new-melting portion and a re-melting portion (the portion within the red line in Fig. 1(b)). In the next layer deposition, the re-melted portion will be melted again to form the initial molten pool for a new top layer and the rest part will be left as an everlasting previous layer of the deposited wall structure.

2.2. Process model of layer deposition width

From the above discussion, it can be concluded that the volume of a top layer V_{top} can be expressed in two ways (as expressed in Eq. (1)).

$$V_{top} = V_{rm} + V_{left} = V_{rm} + V_{nm} = 0.5\pi r^2 L \quad (1)$$

where r is the radius of top layer, L is the length of the single-bead wall, V_{rm}, V_{left} and V_{nm} are the volumes of the re-melting portion, the left portion and the new-melting portion, respectively (as shown in Fig. 1(b)). From Eq. (1), it can be found that the volume of the left portion equals to that of the new-melting portion, as expressed in Eq. (2).

$$V_{left} = V_{nm} \quad (2)$$

On the other hand, the volume of the new-melting portion V_{nm} is formed by melting powders during one-layer deposition time and can be calculated as:

$$V_{nm} = \frac{u_1 L \dot{m}}{v\rho} \quad (3)$$

where u_1 is powder utilization efficiency, v is scanning speed, $\dot{m}$ is powder flow rate, and ρ is material density. Substitution of Eq. (3) into Eq. (1) yields:

$$V_{rm} = 0.5\pi r^2 L - \frac{u_1 L \dot{m}}{v\rho} \quad (4)$$

Accordingly, the total energy Q_{total} needed for depositing a top layer can be considered as the sum of the energy for re-melting (Q_{rm}) and the energy for melting powders (Q_{nm}) (Eq. (5)).

$$Q_{total} = Q_{rm} + Q_{nm} \quad (5)$$

According to thermodynamics, we can get the required energy Q_{rm} for re-melting during one layer deposition time:

$$Q_{rm} = Cm_{rm}\left(T_m - T_1\right) + \Delta H m_{rm} \quad (6)$$

where C is the specific heat of fabricated material, $\triangle H$ is the specific latent heat of fusion-solidification, T_m is the melting temperature of fabricated material, T_1 is the temperature of previous layer, and m_{rm} is the mass of re-melted material of one layer which can be defined as:

$$m_{rm} = \rho V_{rm} \quad (7)$$

Similarly, the required energy Q_{nm} for new-melting of one layer can be expressed as:

$$Q_{nm} = Cm_{nm}\left(T_m - T_2\right) + \Delta H m_{nm} \quad (8)$$

where T_2 is the initial temperature of powders and m_{nm} is the mass of new-melted material which can be written as:

$$m_{nm} = \rho V_{nm} \quad (9)$$

Energy transformation during the deposition procedure is extremely complex, but if we take the melt pool as a separate intermediary object, the energy transformation process can be considered as two steps. The first step is energy absorption process, during which the output laser energy is absorbed partly by substrate or previous layer to generate a little melt pool. At the same time, powders feeding into the melt pool also absorb energy by means of radiation of laser beam to be melted and increase the pool volume. The second step happens after the laser beam moving away, and can be called energy dissipating step, during which the melt pool solidify and dissipate previously absorbed energy by means of conduction, convection and radiation to the substrate, deposited layers and the ambience (Niu et al., 2014).

In fact, the energy keeps dissipating through all the deposition procedure, even during the energy absorption step. But compared with energy dissipating process, the previous layer or the newly feeding powder can be considered as being melted instantaneously by laser beam with high power density (Tang and Landers, 2011). Therefore, the energy dissipated in the first step can be neglected and only the energy absorption will be taken into consideration.

On the other hand, the real consumed energy for melting one layer is from the output energy of the laser (Q_{out}) and can be expressed as a function of laser power P and the deposition time:

$$Q_{out} = u_2 PL / v \quad (10)$$

where u_2 is the absorption efficient of laser which is assumed unchangeable during the deposition procedure.

According to the first energy transformation step and the energy balance principle, the total required energy Q_{total} for deposition process equals to the real utilized energy Q_{out} during the same layer, which means:

$$Q_{total} = Q_{out} \quad (11)$$

By substituting Eqs. (3) - (10) into Eq. (11), the deposition width model can be obtained as:

$$w = 2r = 2 \bullet \sqrt{\frac{u_2 P + u_1 C m \& (T_2 - T_1)}{0.5\pi\rho v(CT_m - CT_1 + \Delta H)}} \tag{12}$$

3. Discussion of the deposition width model

From the deposition width model in Eq. (12), it can be concluded that process parameters, physical properties of deposited material and initial conditions are the main three factors influencing deposition width. For a typical LENS procedure, the two latter factors are usually fixed and only the process parameters can be conveniently used for controlling deposition width. The model reveals that deposition width of a single-bead wall structure is related with the laser power, powder flow rate and scanning speed.

3.1. Influence of powder flow rate on deposition width

Because cooling rate in LENS is usually high, the difference between powder initial temperature T_2 and the previous layer temperature T_1 is comparably small. In addition, the magnitude of $\dot{m}$ is generally on the order of 10^{-4} kg/s. As a result, the term $u_1 C \dot{m} (T_2 - T_1)$ in Eq. (12) is much smaller than $u_2 P$ and could be dropped. Then the deposition width model can be simplified as Eq. (13). Clearly, the deposition width is affected little by the powder flow rate. This conclusion agrees well with published experimental results of Bian et al. (2013).

$$w = 2r = 2 \bullet \sqrt{\frac{u_2 P}{0.5\pi\rho v(CT_m - CT_1 + \Delta H)}} \tag{13}$$

While the laser power is held constant which means Q_{total} is fixed value, high powder flow rate results in more powders feeding into melt pool and therefore the deposition height increases. In other words, more energy is consumed for new-melting and less energy is used for re-melting accordingly. On the whole, the volume of melt pool will not change much as a result of constant laser power input. Thus, the deposition width keeps stable with the variation of powder flow rate.

3.2. Influence of scanning speed on deposition width

For given laser power, Eq. (13) can be simplified as Eq. (14) and the relationship between scanning speed and deposition width is revealed clearly.

$$w = \frac{A_1}{\sqrt{v}} \tag{14}$$

where A_1 is constant depending upon other process parameters and the properties of deposited material. As the results reported by many experimental studies, the deposition width decreases with increasing of

scanning speed. However, the exact numerical relationship between them is that the deposition width is inversely proportional to $v^{1/2}$.This is because it spends less time on scanning unit length with faster travel speed and fewer powders are fed into melt pool accordingly. Meanwhile, energy input decreases for unit length because scanning time becomes less. As a result, the faster the scanning speed, the smaller the melt pool is, and therefore the narrower the deposition width.

3.3. Influence of laser power on deposition width

Similar with the scanning speed, if other process parameters and deposited material are fixed, the relationship between deposition width and laser power can be simplified as Eq. (15):

$$w = A_2\sqrt{P} \tag{15}$$

where A_2 is constant depending upon other process parameters and the properties of deposited material. With simplify of the model, it becomes clear that the layer deposition width have a linear relation with square root of laser power $P^{1/2}$. Similar with decreasing scanning speed, more laser energy will be input in unite length when the laser power increases, which results in larger molten pool and deposition width.

4. Experimental verification

Experiments of fabricating single-bead wall structures with 316L stainless steel are designed and conducted by a LENS system to verify the conclusion revealed by the deposition width process model. The LENS system mainly consists of a 4000 W semiconductor laser, a two-container powder feeder and an articulated robot. 99.9% pure argon was used for sending powders and shielding the deposited specimen. The laser beam and powder flow are output from a coaxial spray nozzle fixed at the end of the robot.

316L stainless steel powders were used for these experiments and dried in 100 ℃ oven for 4 hours so as to remove vapor before depositing. 12 single-bead wall specimens were fabricated in 3 groups, as shown in Table 1. In each group, the laser power, scanning speed and powder flow rate vary in proportion separately. Z-increment and deposition number are accordingly set for every specimen. Finished wall structures were cut from the longitudinal cross-section and Vernier caliper were used to measure the specimen width.

Table 1. Process parameters and experimental results for the 12 specimens.

Group number	Specimen number	Laser power (W)	Scanning speed (mm/s)	Powder flow rate (g/s)	Calculated deposition width (mm)	Measured deposition width (mm)	Relative error (%)
1	1	1000	6	0.089	3.67	3.60	1.9%
	2	1000	6	0.133	3.67	3.76	2.4%
	3	1000	6	0.177	3.67	3.70	0.8%
	4	1000	6	0.222	3.67	3.84	4.6%
2	5	500	6	0.133	2.58	2.70	4.7%
	6	1000	6	0.133	3.67	3.70	0.8%
	7	1500	6	0.133	4.48	4.56	1.8%
	8	2000	6	0.133	5.18	5.28	1.9%

3	9	1000	4	0.133	4.48	4.12	8.0%
	10	1000	6	0.133	3.67	3.60	1.9%
	11	1000	8	0.133	3.17	3.24	2.2%
	12	1000	10	0.133	2.84	2.86	0.7%

Cross-section of every specimen is shown in Fig. 2-Fig. 4. Calculated deposition width and measured deposition width are listed in Table 1 and also plotted against each other in Fig. 5. To estimate the accuracy of the proposed model, relative error is calculated in Table 1.

Table 1 show that the relative error of each specimen is basically below 5%. It appears form Fig. 5 that the real width of the fabricated specimens agrees well with the theory value calculated by the process model Eq. (13). It is evident form the experimental results that the deposition width is significantly affected by laser power and scanning speed, but not by the powder flow rate. In addition, the deposition width increases with increasing of laser power, and the increasing rate accords with the relationship revealed in Eq. (15). On the other hand, with the proportional increasing of scanning speed, deposition width decreases accordingly as the Eq. (14). The experimental results indicate that the proposed process model is accurate and relationships revealed by it between deposition width and process parameters can be used for dimensional controlling in LENS.

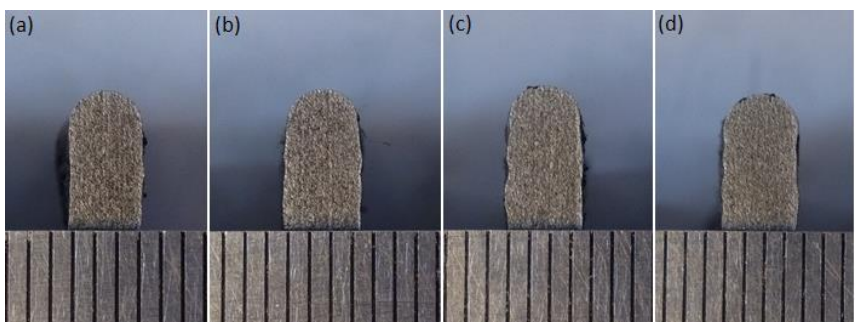

Fig. 2. Specimens of Group 1: (a) specimen 1, (b) specimen 2, (c) specimen 3, (d) specimen 4

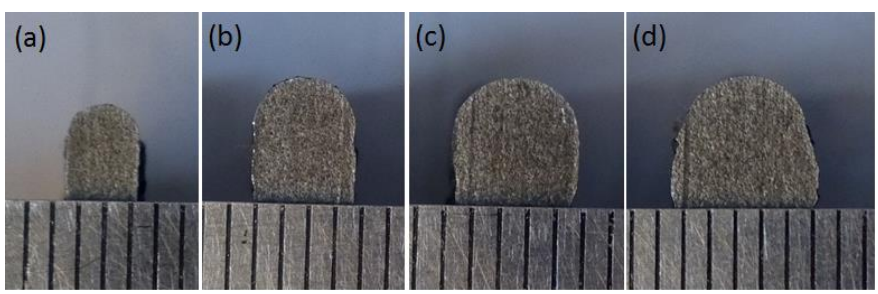

Fig. 3. Specimens of Group 2: (a) specimen 5, (b) specimen 6, (c) specimen 7, (d) specimen 8

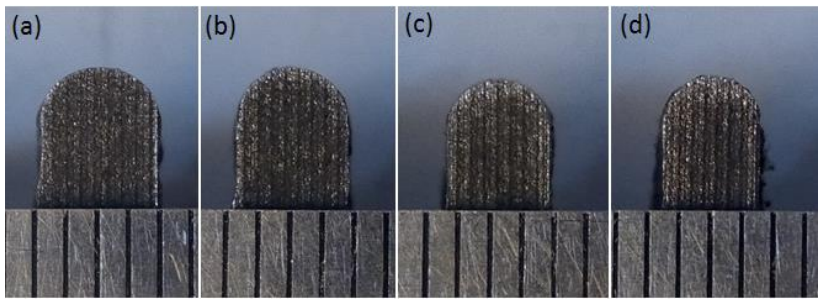

Fig. 4. Specimens of Group 3: (a) specimen 9, (b) specimen 10, (c) specimen 11, (d) specimen 12

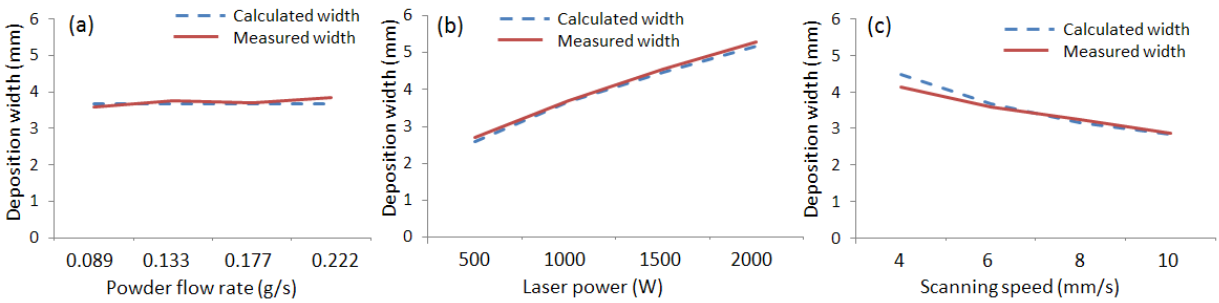

Fig. 5. Comparison of the calculated width and measured width: (a) results of group 1, (b) results of group 2, (c) results of group 3

5. Conclusions

In this study, typical layer-by-layer deposition procedure of LENS was illustrated. According to the analysis, deposition width process model was deduced on the basis of volume and energy balance principles. With the aid of the model, relationship of process parameters and deposition width was discussed quantitatively. Deposition width are mainly affected by laser power and scanning speed, while affected little by the powder flow rate. It is revealed that the deposition width is proportional to the square root of laser power, while inversely proportional to the square root of scanning speed. The relationships between deposition width and process parameters were verified by fabrication of 316L stainless steel single-bead wall structures. The experimental results agree well with calculated value by the proposed model.

Acknowledgements

The authors would like to acknowledge the financial support from the National Nature Science Foundation of China (No.51175061, No.51402037), the Science Fund for Creative Research Groups (No.51321004) and the National Key Basic Research Program of China (No. 2015CB057305).and the China Postdoctoral Science Foundation Funded Project (No.2014M551072).

References

Atwood, C., Ensz, M., Greene, D., 1998. Laser engineered net shaping (LENS(TM)): A tool for direct fabrication of metal parts. Sandia National Laboratories, Albuquerque, NM, and Livermore, CA.

Arcella, F., Froes, F., 2000. Producing titanium aerospace components from powder using laser forming. Jom 52, p. 28.

Bandyopadhyay, A., Krishna, B.V., Xue, W., Bose, S., 2009. Application of laser engineered net shaping (LENS) to manufacture porous and functionally graded structures for load bearing implants. J. Mater. Sci. Mater. M. 20, p. 29.

Bian, H., Wang, T., Wang, W., Yang, G., Qin, L., Cui, B., 2013. Effect of process parameters on both molten pool temperature and layer size during metal laser deposition shaping. Applied Laser 33, p. 239.

De Oliveira, U., Ocelik, V., De Hosson, J., 2005. Analysis of coaxial laser cladding processing conditions. Surface and Coatings Technology 197, p. 127.

Li, Y., Yang, H., Lin, X., 2003. The influences of processing parameters on forming characterizations during laser rapid forming. Materials Science and Engineering: A 360, p. 18.

Keicher, D., Smugerrsky, J., Romero, J., 1997. Using the laser engineered net shaping (LENS) process to produce complex components from a CAD solid model. International Society for Optics and Photonics, San Jose, CA, p. 91.

Mazumder, J., Dutta, D., Kikuchi, N., Ghosh, A., 2000. Closed Loop Direct Metal Deposition: Art to Part. Opt. Laser. Eng. 34, p. 397.

Niu, F., Wu, D., Zhou, S., 2014. Power Prediction for Laser Engineered Net Shaping of Al_2O_3 Ceramic Parts, J. Eur. Ceram. Soc. 34, p. 3811.

Srivastava, D., Chang, I., Loretto, M., 2000. The optimisation of processing parameters and characterisation of microstructure of direct laser fabricated TiAl alloy components. Materials & Design 21, p. 425.

Tang, L., Landers, R., 2011. Layer-to-layer height control for laser metal deposition process. Journal of Manufacturing Science and Engineering 133, p. 021009.

Zhang, K., Liu, W., Shang, X., 2007. Research on the processing experiments of laser metal deposition shaping. Opt. Laser. Technol. 39, p. 549.